2007 IEEE International Conference on
Robotics and Automation
Roma, Italy, 10-14 April 2007

Design Tradeoffs for Electrothermal Microgrippers

Mohammad Mayyas, Ping Zhang, Woo H. Lee, Panos Shiakolas, and Dan Popa

Abstract— **Microgrippers based on electrothermal actuation were designed and fabricated using the Deep Reactive Ion Etching (DRIE) process with 100µm thick silicon on insulator (SOI) wafer. The design requirements are restricted to basic manipulation tasks such as pick and place, and nonprehensile manipulation. This paper explores several electrothermal end-effectors which have been fabricated for serial and parallel microassembly. The end-effectors include three main building blocks: 1) Integrated and symmetrical actuators of V and U shapes. The symmetrical expansions on Chevron and hot arms allow combination of forward translations that amplify angular motion at the tips of a gripper. 2) A joule heating element based on a resistive V-shape electrothermal actuator. In 3D microassembly, the joining of a micropart is essentially performed by providing an integrated microheater device. 3) A force or position feedback sensing block based on self-straining or electrostatic principle. The integrated sensor can be calibrated for both position and force measurements. Serial heterogeneous assembly of meso and micro-scale objects is demonstrated using a 3D microassembly station. Black-box dynamical models for microgrippers are derived using experimentally obtained data, and performance variations due to the way the microgrippers are mounted onto the robot are discussed.**

I. INTRODUCTION

The development of micromachining technologies has provided wide applications in micro sensing and actuation. Integrating and packaging of a MEMS device in electronic circuits have been demonstrated [1]. However, most of the demonstrated devices are selectively constructed by fabrication processes that are limited to complexity, configuration, dimension, and material variation. A monolithic fabrication has limitations and does not allow the inclusion of multiple components of incompatible processes. Therefore, the construction of 3D microstructures by heterogeneous microassembly is an alternate manufacturing route [2]. During assembly, numerous methods for controlling the pick and place operations have been utilized in the past. Such techniques include: vacuum grippers based on micro-pipettes [3]; manipulators with heated micro holes acting as suction cups [4]; electrostatic force control method [5]; tweezers "grippers" and teleoperated assembly [6]; moisture and surface tension control methods [7]; and roughness change method and force controlled grasping based on an AFM (atomic force microscopy) [8].

A number of standard MEMS fabrication processes could be utilized to fabricate microgripper devices such as LIGA, SOI, MetalMUMPs, PolyMUMPs, FIB, EBL and DRIE [6, 9]. Electrothermally (E-T) driven micromechanical devices are based on asymmetrical thermal expansion, and led to the development of many microactuators [10, 11]. This actuation principle is capable of providing larger deflections and forces compared to electrostatic, piezoelectric, and magnetic actuation [12]. However, high power requirements of typical E-T building blocks such as Chevron, bimorph and monomorph thermal actuators often causes thermal failures and limits operating force, operating deflection, operating structural frequency, and the bonding conditions at the device's pads. Thus careful design tradeoffs must be followed for practical use of E-T devices in microassembly.

In this paper we study such trade-offs for E-T microgrippers and exemplify how these end-effectors can be fabricated, modeled, and attached onto precision robots for heterogeneous microassembly.

The organization of this paper is as follows: in Section 2 microassembly techniques are briefly classified in order to bring E-T tradeoffs into context. In Section 3 relevant manipulation tasks for E-T devices are discussed. In Section 4 issues pertaining to attaching and operating the microgrippers are discussed. In Section 5, experimental microassembly results are illustrated. In Section 6, black-box models for microgrippers are derived from experimental data. Finally, the paper concludes by addressing practical challenges related to reliable gripper attachment.

II. CLASSIFICATION OF MICROASSEMBLY

Key issues in designing microrobotic end-effectors have been discussed in many prior papers (for instance [2] and [3]), and they stem from:

1) *Precision requirements:* A meso range of workspace must be combined with submicron resolution and micron-range positioning accuracy.
2) *Throughput requirements:* Throughput is determined by the amount of parallel or sequential process flow and the complexity of the assigned assembly tasks.

Manuscript received January 31, 2006. This work was conducted in collaboration with the Bennington Microtechnology Center under the support of Grant # N00014-05-1-0587 from the Office of Naval Research.

The authors are with the Automation and Robotics Research Institute (ARRI), at the University of Texas at Arlington, Fort Worth, TX 76118 USA.

M. A. Mayyas (e-mail: mayyas@uta.edy) and Ping Zhang are pursuing their doctorate studies in Mechanical and Electrical Engineering, respectively, in the area of microrobotics.

Dan O. Popa, Ph.D., (also corresponding author) is currently an Assistant Professor of Electrical Engineering (e-mail: popa@arri.uta.edu). His research interests include multiscale and microrobotics, 3D microsystems integration, embedded and distributed sensors and actuators.

Panos Shiakolas, Ph.D. is Associate Professor of Mechanical Engineering. His research interests include robotics & mechatronics, bioMEMS and precision micromanufacturing.

Woo Ho Lee, Ph.D., is currently a research faculty member with ARRI (email: whlee@arri.uta.edu). His research interests include MEMS design and fabrication, active surface devices, and modular robotics.

1-4244-0602-1/07/$20.00 ©2007 IEEE.

3) *Sensory vs. sensorless ability:* Sensory feedback to monitor and guide manipulation tasks is achieved through vision systems, prehensile positioning and force sensing. Sensorless assembly, on the other hand, is often guided by the "self-assembly" concept, geometrical constraints, or open-loop control.

Microassembly can accordingly be classified into:

1) *Deterministic microassembly*: several semi or fully automated workcells guided by vision, force and position feedback have been proposed. The control system architecture with integrated part handling from CAD layout enables performing complex manipulation tasks. Deterministic microassembly can also be classified into serial and parallel assemblies:
   a. Depending on *a priori* microparts organization, *parallel microassembly* enables a large number of parts to be assembled simultaneously with micro-scale precision.
   b. *Serial microassembly* or commonly called "pick and place" requires the well defined infrastructure of an end-effector and a micropart to interface with each other. The process is often limited to stiction forces and is time-consuming.
   c. *Exponential assembly:* This technique was introduced in [19] and refers to ever-increasing numbers of assembled copies.
2) *Stochastic microassembly*: A large number of distributed microparts is spontaneously or algorithmically organized either by:
   a. *Distributed arrays* of MEMS sensors and actuators: Such arrays include distributed manipulators which dynamically recruit the fixed neighborhood modules to work together [13, 14].
   b. *Self-assembly* which is inspired by nature: Examples include biomimetic systems [9], fluidic assembly [1] based on capillary, van der Waals, and electrostatic forces [1, 7, 5].
3) *Hybrid microassembly*: This is defined as the process of combining the aforementioned techniques to perform the desired tasks.

In this research work, we use MEMS-based E-T microgrippers as end-effectors for a robotic manipulator workcell that is deterministic in nature. The μ^3 microassembly system at the Texas Microfactory™ is composed of a set of three precision robots with a total of 19 DOFs. The μ^3 is shown in Figure 1 and described in more detail in [20]. The μ^3 has been used to demonstrate mainly serial microassembly processes. However, parallel and exponential microassembly, as well as hybrid microassembly have also been demonstrated on the μ^3 platform. We pursue an integrated end-effector design, thus accomplishing several tasks at once, such as active gripping, heating, and force sensing.

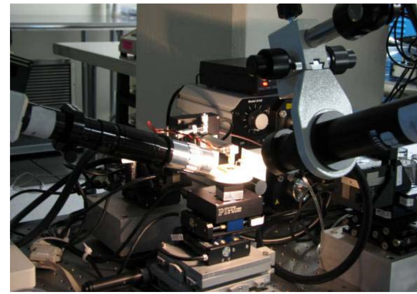

Fig. 1. μ^3 microassembly system with three precision robots and stereo microscope vision.

III. MICRO-PART HANDLING REQUIREMENTS

Generally, automated task execution in assembly is used to ensure robust assembly and a short cycle time. These are desirable capabilities in microassembly as well. In addition, basic manipulation tasks, such as pick and place, and nonprehensile manipulation are generally restricted to specific objects. The design of an end-effector should consider the complexity of tasks that can encompass, for instance grasping, pushing, flipping, throwing, squeezing, twirling, smacking, blowing, and heating. Our E-T designs are themselves "in-plane" 2½D microparts intended for the following operations:

1- **Pick and place of heterogeneous microparts** via friction (Silicon MEMS and non-Si MEMS). Examples of such designs are shown in Figure 2.

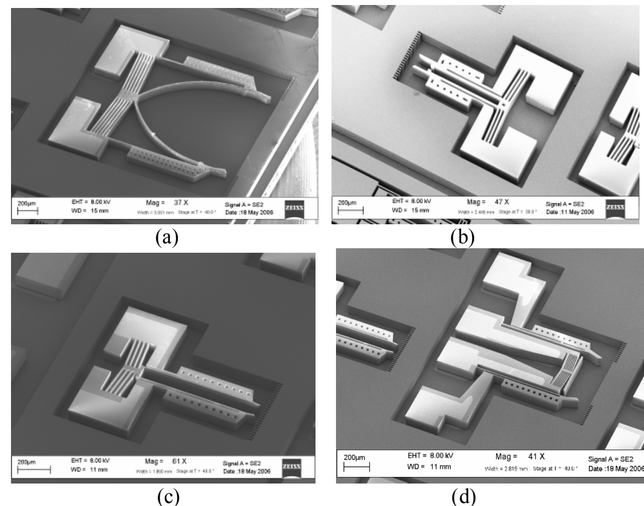

Fig. 2. Electrothermal microgrippers: (a) Stiff gripper for manipulation of 1000µm cubic blocks. (b) Active gripper with 90 µm nominal opening and low out of plane stiffness. (c) Active microgripper with 90µm nominal opening and high out of plane stiffness. (d)Microheater embedded microgripper with nominal opening of 240µm.

Heterogeneous assembly is accomplished by manipulating microparts with such processes as remove, insert, grasp, place, push, pull, translate and orient from their substrates on a chip and join them to other micro-parts at a secondary location. For the microgrippers in Figure (2-a, b, and c), the mechanical structure is composed of two basic building blocks: first a V-shape actuator or "chevron" whose apex moves forward as a result of the symmetric thermal

expansion of the chevron beams; and second, the U-shape structure or "folded beam" is based on the asymmetrical thermal expansion of connected beams. The narrow arm "hot-arm" pushes the wider arm "cold-arm" and causes the block-tip to deflect causing a wider opening. The meso-micro scale gripper in Figure (2-a) has a nominal opening of 960µm and it possesses high in plane stiffness which prevents the picked parts from sliding in a noisy translation. Meanwhile the microgripper in Figure (2-b) has 90µm nominal opening and it is optimally designed to provide wide tip opening at low temperature profile. The microgripper structure in Figure (2-c) has larger opening and better out of plane stability than that on Figure (2-b). This enhancement though comes at the expense of the thermal budget which tends to cause much higher temperature at the chevron symmetrical axis.

2- **Joule heating source for joining of microparts.** A resistive V-shape microactuator does not only transfer heat flux to the mated micropart, but also provides external uniform bonding pressure through the translation of the apex. By utilizing a microheater building block soldering or welding processes for various applications such as a joint for a 3D microstructure could be achieved. In addition, the applied pressure and the heat conducted to the micropart could be utilized as a "controlling parameter" during micropart release in overcoming the inherent adhesive forces between the micropart and the contact surfaces of the tip of the gripper.

Figure (2-d) shows a multipurpose E-T MEMS gripper with combined capabilities: 1) basic pick up and place achieved by the symmetrical opening of the compliant double-U thermal actuator; 2) heat generation element provided by the dense V-beams causing heat to conduct into the mating surface; 3) the axial deflection in the chevron actuator exerts an external force causing a firm contact between the micropart and a substrate.

3- **Sensory feedbacks to control, guide, and observe manipulation tasks.** Embedded sensor elements can be calibrated to measure not only the in-plane and/or out of plane deflection of MEMS end-effectors but also the reaction forces which are caused during assembly. The MEMS actuator in Figure 3 can perform simultaneously three tasks; pick and place, heating and sensing. The feedback sensing is based on the resistivity changes of the highly doped silicon [15]. In this work, the electrothermal or external forces/deflection cause elastic straining in the dual spring.

4- **Other types of operations to revert or enhance parts handling.** Examples include design of E-T micro-tweezers and complex integration of multiple E-T blocks. The opening direction of a tweezer in Figure (4-a) is the inverse of a normal gripper. Part picking is either performed by 1) passive insertion under which the gripper is inserted with non-zero contact force and zero input voltage; or 2) active picking with zero insertion force. Figure (4-b) shows integrated V and U-shape actuators with an embedded microheater.

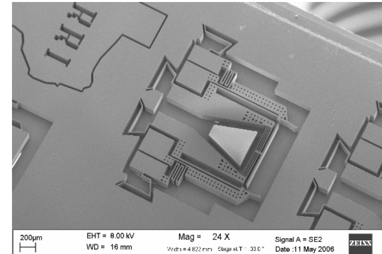

Fig.3. Novel design of electrothermal actuator of 960µm nominal opening: integrated microgripper, microheater and embedded strain sensor.

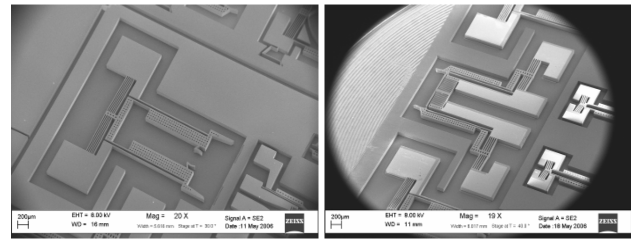

(a) (b)

Fig. 4. Miscellaneous electrothermal MEMS devices: (a) Microtweezer "inverted microgripper". (b) Novel microheater and an integrated microgripper with V and U shape mechanisms.

IV. E-T DEVICE HOLDER REQUIREMENTS

The complexity of introducing MEMS devices into the 3D microassembly workcell is illustrated by the need of providing electrical interconnection to their pads. A rigid double layer holder is thus interfaced between the microgripper and the manipulator of μ^3 system. A high performance holder essentially provides a package for the interconnected microgrippers and requires mechanical, chemical and thermal stability. As a result, ceramic or silicon plates are candidate holder materials, rather than traditional circuit board layers which are easily warped and melted.

Our E-T devices have three pad arrangements (2, 4 and 6). A ceramic holder with gold traces shown in Figure (5-a) is suggested. Several techniques can be deployed to firmly attach pads to the holder, which provides a low resistance at electrical interconnections:

1. Applying thermal epoxy at the attachment area of a ceramic face. The microassembly stage is utilized to align and position the gripper relative to the holder. Curing the bonds at prescribed temperature is established by using a hot plate. Next step is to perform wirebonding between traces and gold coated pads on the MEMS gripper.
2. Applying electrical conductive epoxy on holder trace. The actuator is then aligned and attached electrically and mechanically at the same time as shown in Figure (5-b).

After assembling packaged end-effectors, the E-T device can be externally excited by regulating the voltage according to the following classifications:

1) *Two pads arrangement:* E-T device requires [0, V] excitation mode. An example is the combined Chevron and bimorph gripper as shown in Figures (2 and 4-a).

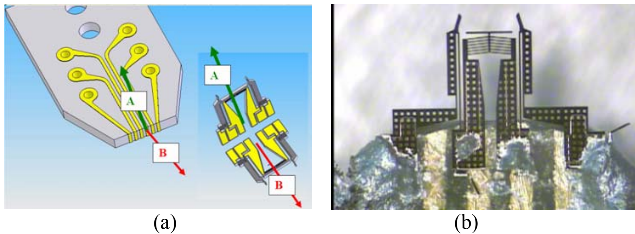

(a) (b)

Fig. 5. Adapter for interfacing E-T device to 3D microassembly station: (a) Ceramic holder with 6 interconnections. (b) A released E-T device is attached to the ceramic holder by conductive epoxy.

2) *Four pads arrangement*: E-T devices in Figures (2-d and 4-b), allow two modes of actuation mechanisms.

a) Sequential excitation of actuators is easily applied by choosing to operate either the gripper or heater. In this case the pads are excited as follows:

i. To excite gripper alone we chose the following strategy: [V-0-0-V] or [0-V-V-0], where V is the voltage excitation corresponding to pad sequence, i.e. from right to left (1-2-3-4).

ii. To excite only the microheater/microstroke requires passing power to the chevron beam by the following mechanism: [0-V-0-0] or [0-0-V-0] where V is the voltage supplied across the microheater pads according to the following sequence (1-2-3-4).

b) Simultaneous excitation of heater and gripper is obtained by feeding the four pad with the following sequences:

i. [0-V-0-V] to provide same voltage for both actuators.

ii. [0-V-(-V)-0] or [0-(-V)-V-0] to provide double voltage to heater relative to gripper.

iii. [V-0-V/2-(-V/2)] to provide double voltage across the gripper relative to heater.

V. MICROASSEMBLY APPLICATIONS UTILIZING E-T ACTUATORS

In this section, we demonstrate the use of E-T microgrippers for heterogeneous microassembly. The robots within μ^3 microassembly system bridge the dimensional gap between meso, micro, and nano scales. The E-T device is fixed at the end of the flexure arm and attached to a ceramic holder. The silicon pads of E-T device are attached and fixed to the ceramic holder by using conductive silver epoxy.

First, an E-T microgripper is interfaced to μ^3 system. Figure (6-a) shows the E-T device of 960µm nominal opening that is designed to grasp a metal block with dimensions $(1000 \pm e_1 \times 1000 \pm e_2 \times 500 \pm e_3)\mu m^3$.

This gripper operates in two modes: active and passive. Depending on the gripper tip design, an active gripper is electrothermally driven to open and close. It not only allows picking and placing, but also accounts for dimension uncertainty (e_1, e_2) of the picked metal block. On the other hand, the passive gripper demonstrates the ability to grip parts by forced insertion. The stiffness of in plane structure provides reaction and clipping force. Releasing or placing task is performed by actuating the device as depicted in Figure (6-b).

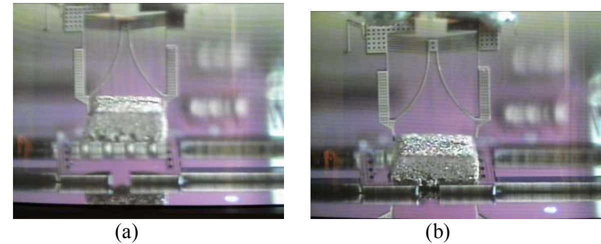

(a) (b)

Fig. 6. Sequential microassembly performed on MEMS die: (a) Pick up a metal block. (b) Placing metal block onto specified site.

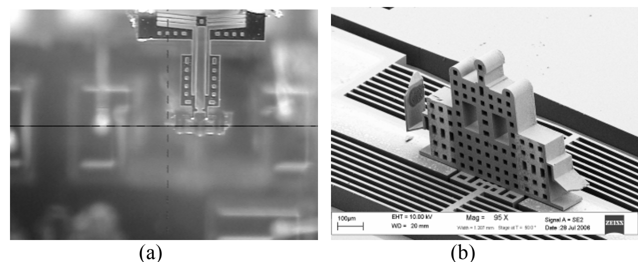

(a) (b)

Fig. 7. Microassembly of a micropart: (a) Top view of a microgripper handling a micropart. (b) Assembling a micropart into a locking mechanism on a MEMS die.

A second demonstration involves fashioning of a micropart "jammer" assembled into the substrate. The E-T gripper tip is designed to grasp the jammer from the neck of etched holes. A top view of the assembly process is shown in Figure (7-a). Such an assembly requires several process sequences: activate the gripper, pick the micropart, locate and position them to the desired assembly site, activate locking mechanisms on an MEMS die, place the micropart, deactivate lock on an MEMS die, and finally activate the microgripper in order to release and place the micropart on its final position as shown in Figure (7-b).

Hybrid microassembly is used at the third experiment, by combining sequential pick and place with E-T grippers for the parallel orientation of microparts on the substrate. The process is summarized as follows:

- A silicon die with etched holes is agitated to trap and orient the distributed micro-meso parts near hole-sites. These sites have local minimum vibration-energy while the unetched surface has higher energy. Figure (8-a and b) shows the "spontaneous" positioning of a $1 \times 1 \times 0.025 mm^3$ metal preform onto the binding sites of an agitated silicon substrate. Piezo-resonators are utilized to create a force field that overcomes stiction to locate at binding site.
- The silicon substrate is fixed in position and thus the process of detecting parts becomes easier and can be automated (Figure (8-c)). Here, the end-effector is translated into binding site to continue the assembly processes.

- Parallel assembly with multiple E-T end-effectors can now be achieved. E-T devices are arranged and embedded on an interface holder as shown in Figure (8-d).

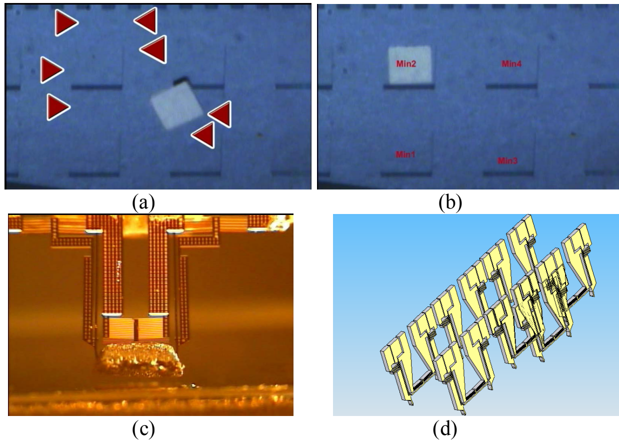

Fig. 8. Hybrid to parallel microassembly: (a) Initial position, the monolithic self-assembly utilizing a piezo based agitation for silicon substrate of etch holes array. (b) Milliseconds after agitating plate. (c) Continuing the sequential assembly on the metal preform which is positioned on Fig. (8-b). (d) Multiple E-T actuators performing parallel assembly.

VI. Dynamic Response Measurement of E-T Microgripper

The E-T MEMS devices can be characterized using measured electro-thermo-elastic responses. We used two methods to extract a “black box” model for the proposed microgrippers: first, parametric identification based on minimization of the prediction error/Maximum Likelihood method; and second, frequency response analysis. The microgripper in Figure (2-b) is *identified* using test signal inputs with 50% duty cycle square shape at amplitude of 16V at frequencies of [20, 70, 100, 180, and 1000] Hz. A 3D MEMS profilometer (WYKO-NT1100) [16] is utilized to measure the static and dynamical deflections of one side of a gripper tip, and they are plotted in Figure (9-a and b). The SISO measurements are identified for several models utilizing MATLAB identification toolbox [17] including ARX, ARMAX, OE and general form models (for more details, see Ljung [18]). Table 1 depicts the good fit at different frequency measurements. The parametric identification for the measured outputs due at 20Hz frequency input is plotted for different models as shown in Figure (9-c). Higher fitting values show better results as they are defined according to the *compare* function of the MATLAB identification toolbox [17]:

$$fit = 100 \times \left(1 - \frac{\| \hat{Y} - Y \|}{\| Y - \bar{Y} \|} \right),$$

where Y is the measurement vector of the gripper tip displacement at one side measured in µm. The simplest representation of a stable continuous transfer function is extracted from OE of order [1 1 1] and at 91% fit:

$$y(t) = \frac{3576}{(s+3535)} V(t) + e(t).$$

Table 1. Good of Fitting at each model of orders: [na,nb,nc,nd,nf,nk]=[2,2,2,2,2,1]

	20Hz	70Hz	100Hz	180Hz	1kHz
ARX	91.8060	95.6334	96.8333	96.4295	86.3838
ARMAX	82.0472	97.6175	98.0074	94.8550	82.1597
OE	3.2239	98.0498	98.3867	96.6863	95.4888
OE**	91.2608	94.8697	96.0809	96.2083	86.1107
BJ	78.6741	98.4945	97.7333	96.1127	96.4152
GF	92.0422	97.2156	96.7365	94.6612	85.4628

** The output error order is modified into[1 1 1].

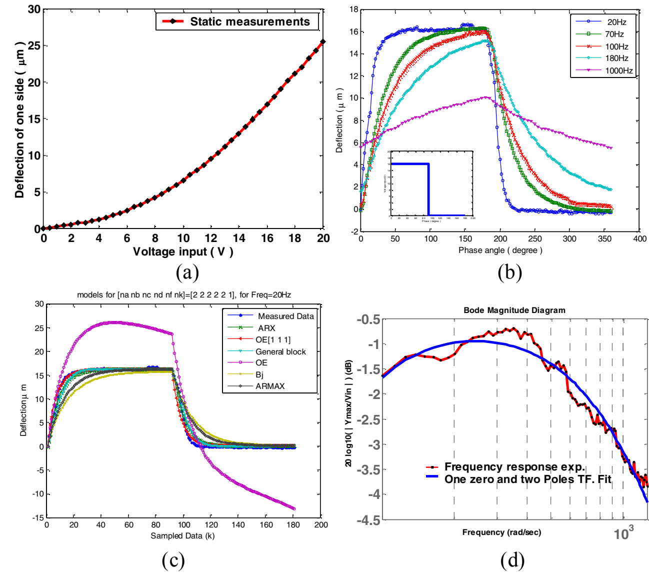

Fig. 9. Dynamic response of the microgripper, in Figure (2.b), attached to silicon substrate. (a) Static DC input voltage vs. deflections. (b) The measured deflection responses of one side of gripper tip under square excitation signals and with several frequencies. (c) Estimated tip deflections utilizing several structures and for the sampled measurements under 20Hz square voltage input. (d) Frequency response analysis.

Figure (9-b) shows that for this attached microgripper, the maximum operating frequency at which it will recover a full structural cycle (no heat accumulation) is 100Hz.

The frequency response of an E-T microgripper is more informative in identifying the dynamics of a system. A gain curve Bode plot for the microgripper is established by measuring the dip deflection response to pure sinusoidal voltage input, *V(t)*. In Figure (9-d), the deflection response, *Y*, of the dip deflection, is plotted for a desired frequency range from 16Hz to 200Hz. It is clear that the response starts damping (roughly as 20 dB/decade) after approaching resonant frequency of 52Hz, hence a first order model is adequate for a good fit. It is important to note that different gripper designs may require higher order models and different model fits at various frequency ranges due to lower resonant frequencies and more nonlinear characteristics.

VII. Challenges and Alternative Solutions

The voltage drop associated with contact resistance at the E-T gripper contact pads becomes an important issue

because of the generated heat. This is apparent for E-T devices that require especially large input power. As a result, the microgrippers become unreliable after repeated operations, or debonded from the holder. We illustrate challenges for the microgripper in Figure (2-a) whose characteristics were evaluated by parabolic shape static deflection with single side opening of 10µm at 23V, damping deflection in the range of 15-150Hz and resonance frequency at 120Hz. Although electrical conductive epoxy used to attach the gripper has low electrical resistivity, its low melting point can be exceeded when the current drawn by the E-T actuator is large. Accordingly, the overall resistance and mechanical resonance of the E-T gripper varies during continuous or intermittent operation. Solution can be addressed by:

- We can reduce the pad resistance by coating the pad area with metal layers. In addition, coat the entire device face with metal. A 20nm thick chromium layer and a 100nm thick gold layer are used. This metal coat decreases the device power consumption and increases the linear ranges of total resistance. On the other hand, the short circuit, which is caused by metal layers, is disconnected at point that possesses a high melting point. This phenomenon is observed at the longest and the narrowest arm of the microgripper. For a released microgripper operating in an ambient environment, the coated gripper has saturated at 16.33V and 0.156Amp. Meanwhile current of the uncoated gripper saturates at a higher value of 23.4V and 0.274Amp. At saturation, the corresponding openings of uncoated and coated are 22µm and 16µm, respectively. Obviously, drawbacks in a metal coated silicon microgripper include early current saturation which decreases the deflection.
- An alternative design introduces the package during fabrication process, by fabricating the holder itself out of silicon with DRIE. Figure (10) shows the design of a multipurpose E-T actuator that is attached on the silicon substrate. This device has the capability of combined V and U actuation mechanisms for gripping, V shape resistive heating element and a reliable electrostatic feedback sensor.

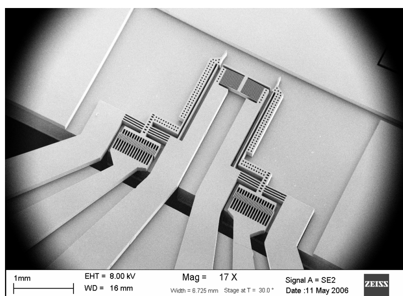

Fig. 10. SEM picture of an E-T silicon microgripper with a holder.

VIII. CONCLUSIONS AND FUTURE WORK

This paper discusses tradeoffs in design, fabrication, packaging and use of electrothermal MEMS devices for microassembly applications. Examples of E-T end-effectors are fabricated containing three basic design building blocks: actuation mechanisms, heating elements, and feedback sensor blocks. The dynamical performance of packaged end-effectors was assessed. Practical challenges in attaching and exciting E-T devices were also discussed. Future work includes the formulation of an expert system for design, fabrication, packaging and use of E-T microgrippers, and formulation of exponential and parallel assembly.

REFERENCES

[1] K. F. Böhringer, "Surface Modification and Modulation in Microstructures: Controlling Protein Adsorption, Monolayer Desorption, and Micro-Self-Assembly," *Journal of Micromechanics and Microengineering,* Vol.13, pp. 1971-1988, July 2003.

[2] M. B. Cohn, K. F. Böhringer, J. M. Novorolski, A. Singh, C. G. Keller, K. Y. Goldberg, R. T. Howe, "Microassembly Technologies for MEMS," *SPIE Conf. on Micromachining and Microfabrication Process Technology IV*, pp. 2-16, Santa Clara, CA, September 1998.

[3] T. Sato, K. Koyano, M. Nakao, and Y. Hatamura, "Novel Manipulator for Micro Object Handling Interface between Micro and Human Worlds," *Proc. of IEEE/RSJ Int'l Conf. on intelligent Robots and Systems*, pp. 1674-1680, 1993.

[4] F. Arai and T. Fukuda, "A new pick up and release method by heating for micromanipulation," *Proc. of IEEE tenth annual international workshop on MEMS '97*, pp. 383-388, 1997.

[5] J. T. Feddema, A. J. Ogden, L. K. Warne, W. A. Johnson, D. Armour, "Electrostatic/electromagnetic gripper for micro-assembly," *World Automation congress, Proc. of the 5th biannual*, pp. 268-274, 2000.

[6] W. Riethmuller and W. Benecke, "Thermally excited silicon microactuators," *IEEE Trans. on Electron Devices*, Vol. 35, Issue 6, pp.758–763, June 1988.

[7] P. lambert, P. Letier, and A. Delchambre, "Capillary and surface tension forces in the manipulation of small parts," *Proc. of the 5th IEEE int'l Sympo. on assembly and task planning*, pp. 54-59, 2003.

[8] Y. Zhou and B. J. Nelson, "The Effect of Material Properties and gripping forces on micrograsping," *Proc. of IEEE int'l conf. on robotics and automation*. pp. 1115-1120, 2000.

[9] S. E. Lyshevski, *MEMS AND NEMS, Systems, Devices, and Structures*, 1st Ed., CRC PRESS, 2002.

[10]J. T. Butler, V.M. Bright, and W. D. Cowan, "Average power control and positioning of polysilicon thermal actuators," *Sensors and Actuators*, Vol. 72, pp. 88–97, 1999.

[11]A. A. Geisberger, N. Sarkar, M. Ellis, and G. D. Skidmore, "Electrothermal properties and modeling of polysilicon microthermal actuators," *J. of Microelectromechanical Systems*, Vol. 12(4), pp. 513–523, 2003.

[12]Que, L., Park, J.-S., Gianchandani, Y.B., "Bent-beam electro-thermal actuators for high force applications," Microelectromechanical systems (MEMS), *IEEE International Conference*, pp. 31–36, 1999.

[13]J. Reiter, M. Terry, K. F. Böhringer, J. W. Suh, and G. T. A. Kovacs, "Thermo-bimorph Microcilia Arrays for Small Spacecraft Docking," *ASME Int'l Mechanical Eng. Congress and Expo.*, pp. 57-63, 2000.

[14]K. F. Böhringer, V. Bhatt, and K. Goldberg, "Sensorless Manipulation Using Transverse Vibrations of a Plate," *IEEE Int'l Conf. on Robotics and Automation*, pp. 1989-1996, May 1995.

[15]Y.B. Gianchandani and K. Najafi, "Bent-Beam Strain Sensors," *IEEE J.* of *Microelectromechanical Systems*, Vol. 5, pp. 52-58, March 1996.

[16]3D MEMS profiler, "WYKO NT1100" www.veeco.com .

[17]MATLAB 7.2, The MathWorks Inc, http://www.mathworks.com/.

[18]L. Ljung, *System Identification*, second edition, Prentice Hall, 1998.

[19] G. D. Skidmore, E. Parker, M. Ellis, N. Sarkar, and R. Merkle, " Exponential Assembly," *Nanotechnology*, 12, pp. 316-321, 2001.

[20] A. D. Das, P. Zhang, W. H. Lee, and D. Popa, "µ³: Multiscale, Deterministic Micro-Nano Assembly System for Construction of On-Wafer Microrobots," *IEEE International Conference on Robotics and Automation,* Rome, Italy, 2007.